



Olive yield monitor for small farms based on an instrumented trailer to collect big bags from the ground

Sergio Bayano-Tejero¹ · Francisco Márquez-García¹ · Daniele Sarri² · Rafael R. Sola-Guirado^{1,3} 

Accepted: 12 September 2023 / Published online: 12 October 2023

© The Author(s), under exclusive licence to Springer Science+Business Media, LLC, part of Springer Nature 2023

Abstract

Fruit logistics during harvesting involves a large-scale deployment of material and human resources. In olive groves and, for small producers, the operation can be carried out in different ways, however, none of these allow a production monitoring or traceability of the harvested fruit. This study presents a compatible methodology with the usual harvesting logistics employed for harvest monitoring. The procedure uses a mechanical system for loading and unloading big bags of fruit weighing approximately 200 kg with a loading arm that can be adapted to a conventional trailer. An electronic system connected to a cloud application is installed on the trailer for geo-referenced recording of the yield. Tests to determine the accuracy of the Global Navigation Satellite System (GNSS) reported values of around 19 mm and 590 mm for the system with and without corrections, respectively, using the Networked Transport of RTCM via Internet Protocol (NTRIP). The error determination tests of the loading bolt weighing system showed high accuracy and linearity with a mean absolute error of 1.1 ± 0.99 kg. The complete system was tested in a traditional olive grove and an intensive olive grove. The harvest maps generated allowed the yield visualisation and to keep a traceability record of the harvested fruit batches. Application of the proposed methodology and systems presents a reduced operation time between loading and unloading of consecutive fruit batches (~2.5 min). The proposed system would be useful for small producers with limited resources who need to control production and fruit traceability on their farm.

Keywords Loading bolt · GNSS · Mechanical harvesting · Yield map · Cloud · Small producers

✉ Rafael R. Sola-Guirado
ir2sogur@uco.es

¹ R.G. AGR 126 “Mechanization and Rural Technology”, Cordoba, Spain

² Biosystem Engineering Division, Department Agricultural, Food Production and Forest Management, University of Florence, Piazzale Delle Cascine 15, 50144 Florence, Spain

³ Department of Mechanics, University of Cordoba, Ctra. Nacional IV, Campus Rabanales, 14014 Cordoba, Spain

Introduction

The harvesting process and logistics of harvested fruit is a task that involves a large manual component, which has a significant impact on crop profitability (Ampatzidis et al., 2014). The way this operation is carried out differs depending on crop type. The most common method is that in which the fruit is harvested manually or mechanically from the trees and deposited in different storage systems such as small boxes, nets or big bags that are left on the ground close to the harvesting location (Ampatzidis and Vougioukas, 2009). These storage systems are loaded onto a trailer or other system that travels around the plot, and either taken to a location with a higher loading capacity or transported directly to the processing industry.

The procedure described above has two fundamental problems. On the one hand, when the harvest is unified in a single storage system such as a trailer, it is difficult to trace the fruit harvested at different locations on the plot. On the other hand, as there is no record of each harvested batch, it is not possible to ascertain the production of each harvested area for a detailed plot control. These problems can be reduced by using harvesters capable of incorporating recording systems called yield monitors (Fulton et al., 2018). However, due to their high cost, such harvesters are often not used by the small-scale farmers who produce a large amount of fruit for the sector (Plasquy et al., 2019, 2021).

This logistic problem of the fruit harvested by small producers is very common in the case of olive groves. For this crop, the most common technique among small producers is to harvest the fruit on nets, which are then dumped into other systems such as nets or boxes on the ground, or directly into small trailers located in the field (Ferguson, 2006; García and Yousfi, 2006). Finally, the content of the trailers is taken to other, larger capacity, trailers or directly to the industry, with no record of traceability beyond a manual record in a field notebook of the total kilograms of fruit harvested. The harvesting process carried out in olive groves is also frequently employed for other traditional crops. For citrus, it is common to manually harvest the fruit and dump it into big bags situated between the different crop rows in the field. Some research has contributed to the implementation of yield monitors by geo-referencing the big bags (Colaço et al., 2020). For other crops, such as apples or pears, harvesting also involves using small bags, the contents of which are then deposited into larger capacity bins (Guevara et al., 2021; Mizushima and Lu, 2013). The configuration of crops and plots, as well as a lack of machinery for their integral mechanisation, results in a high manual component with the consequent difficulty of implementing harvest control and traceability systems.

Yield monitors are composed of a direct yield measurement element by means of weighing (Maja and Ehsani, 2010) or by indirect estimation methods such as machine vision (Stein et al., 2016), time-of-flight (ToF) sensors (Gené-Mola et al., 2020), volumetric flow (Jadhav et al., 2014), drones with different sensors (Feng et al., 2020), and so on. In addition, weight measurement must be linked to geographical coordinates for which high-precision global navigation satellite system (GNSS) solutions are used to obtain an accurate yield map (Perez-Ruiz et al., 2021). Finally, yield monitors must incorporate a system to record information, either locally or remotely in cloud applications (Ampatzidis et al., 2016). The purpose of a yield monitor is to create yield maps that provide the farmer with information about the production per unit area (Underwood et al., 2016) and help decision-making through differential farm management. These systems are designed for large farms where advanced harvesting mechanisation and fruit logistics is possible; however, they are difficult to adapt to farms with a lower degree of mechanisation and technification such as

those associated with small producers. Moreover, a mapping system for small fields may add complexities to data collection and usage that must be considered to maintain a good proportion of the map usable for decision making (Longchamps et al., 2022).

This work proposes a methodology and an instrumented mechanical logistics system for small producers that allows digital registration of the harvesting procedure and crop traceability. Our development is based on the case of olive groves, although, as the discussion section comments, with adaptation it could be very useful for other crops. The aim of the paper is to present this novel method and show its usefulness as a yield monitor. The following sections provide a detailed explanation of the developed system and its instrumentation, explain the methodology to be followed and show the tests conducted to validate its operation.

Materials and methods

Load handling system

The fruit management system consists of a conventional trailer for fruit storage, equipped with a telescopic hydraulic arm for loading and unloading big bags from the ground. Big bags are standard fruit storage systems that are laid out on the ground and onto which the harvested fruit is deposited. They can be hooked onto a loading system by means of rings at the corners of the bag (Fig. 1-1). The trailer has dimensions of $2200 \times 1300 \times 920$ mm and a capacity for approximately 2000 kg of fruit. The arm, which is controlled by a radio control system (Fig. 1-2), rotates through 220° to enable loading on either the left or right side of the trailer, and can extend up to a length of 3000 mm. At the end of the arm there is



Fig. 1 Components of the yield monitor. **1** Transport trailer, **2** Electronic and hydraulic system for arm control, **3** Implement with loading bolt for weighing fruit, **4** Standard big bag for loading fruit, **5** Electronic system for geo-referencing fruit big bags, weighing and sending data, **6** Wireless electronic system for logistic configuration and visualisation, **7** RTK GNSS antenna

a specially designed, inverted T-shaped implement in steel with two pins to hook the rings (two per pin) of standard big bags with different capacities (Fig. 1-3 and -4). The central part of the implement has a loading bolt installed. This is attached to the top of the implement and locked to prevent it from turning. The lower part of the implement hangs from the load bolt so that the load is always perpendicular to the ground to measure the weight correctly. To unload the big bags inside the trailer, a trigger is operated which releases one of the implement's pins, causing the big bag of fruit to fall by gravity and remain attached by means of the remaining support. The trailer is unloaded through the rear door by gravity thanks to a hydraulic cylinder that tilts the whole unit backwards.

Electronic system

The control and recording system developed consists of an electronic system on board the trailer to weigh and geo-reference the fruit (Fig. 1-5) alongside a wireless electronic system to configure the harvesting method and view the parameters (Fig. 1-6). The core of the electronics system on board the trailer is a microcontroller board (Teensy 4.1, SparkFun Electronics, United States), which is connected via the I²C bus to a high-precision GNSS RTK system (ZED-F9P-02B-00, Ublox, Switzerland) to geo-reference the fruit (Fig. 1-7). Another module weighs the different loaded big bags. It consists of an Arduino microcontroller board (Arduino, Arduino Nano, Italy), a load cell amplifier (HX711, SparkFun Electronics, United States), a load bolt with 5 kN capacity and 0.5 kg resolution (F5301, TECSIS, Barcelona) and a CAN module (MCP2515, Microchip, United States) that sends the weight value to the main board. A radio frequency module (NRF24L01, Nordic Semiconductor, Norway) enables the information flow between the wireless system and the system on board the trailer. This information is sent to the cloud application via a 4G modem (Minilite, Microtik, Latvia). The whole electronic system on board the trailer is powered by its own built-in 12 V DC battery, which is connected to the alternator of the transporting vehicle for charging. The 12 V from the battery are supplied to two DC-DC Step-Down converters that stabilize and transform the voltage to 3.3 V DC and 5 V DC. Thus, the main board and the radio frequency module are powered at 3.3 V DC while the Arduino board and GNSS system are powered at 5 V DC. Only the modem is powered at 12 V DC. The wireless electronic system consists of an Arduino microcontroller board (Arduino, Arduino Pro-Micro, Italy), which communicates via serial bus with an 8" touch display (Nextion, NX8048P, Shenzhen) and another radio frequency module. Everything is powered by 3 rechargeable 4800 mAh batteries and another converter to adapt the voltage to 5 V DC to power the display and the Arduino board. Section 'Harvesting and logistics methodology' explains the configuration of the harvesting logistics, which is carried out by means of the display and sent to the electronic system on board the trailer.

Harvesting and logistics methodology

Achieving harvest registration and traceability with the proposed system requires a harvesting methodology compatible with the systems used. Figure 2 shows the different stages proposed:

- 1) Nets are placed under the trees in the same way as for a normal harvesting process. That is, a net is placed that covers the harvest area on each side of a row of trees. Perpendicu-



Fig. 2 Proposed methodology for use of the yield monitor, adapted to the current logistics system. **1** Pre-placement of nets and big bags to receive olives, **2** Olive harvesting using a trunk shaker over nets, **3** Unloading olives onto big bags, **4** Moving the logistics system to the olive loading points, **5** Weighing olives in big bags and unloading to the trailer, **6** Recording in the application and visualisation of yield by coloured polygon map

lar to where the nets lie, i.e., along a main row of the plot, the big bags are positioned on the ground, centred between the trees.

- 2) The fruit is detached with any harvesting system (Sola-Guirado et al., 2014), and the fruit from each tree falls onto the nets located on either side.
- 3) The fruit in both nets is grouped by manually moving the nets in the direction perpendicular to the main row, towards the location of the big bags, into which it is deposited. The empty nets are laid out in a new location to continue the harvest according to step 1.
- 4) In this way, the fruit contained in each big bag corresponds to approximately half of the trees harvested on both sides of the row. The number of trees must be established manually as described in section ‘Map generation procedure’ below.
- 5) On the other hand, an operator who is not involved in the harvesting process drives the instrumented trailer along the main row where the big bags are and positions the trailer close to the big bags. The operator then controls the telescopic arm to load the fruit onto the trailer by placing the rings of the big bag on the T-arm. When the big bag is suspended and static, pressing a touch button on the display records the weight and geo-references the content. Subsequently, the operator pulls the cable which activates the trigger of the implement, releasing one end of the big bag and allowing the fruit to fall into the trailer. The operator uncouples the remaining rings and removes the empty big bag. Finally, the operator moves the yield monitor to another weighing location and starts the sequence again.
- 6) The system automatically generates the batch and harvest maps on a cartographic basis for consultation in the cloud application. This map is created overlaid with the cartographic map and is based on different polygons (formed by the sectors to be harvested) which are coloured according to a scale of the weight of the batch per area harvested.

Fig. 3 Interface developed for logistics configuration and parameter visualisation

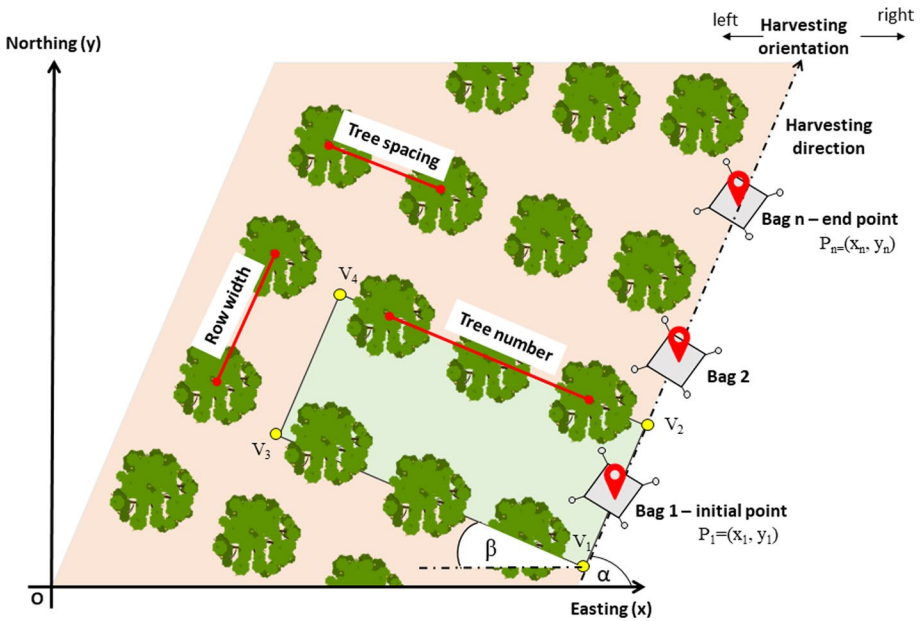


Fig. 4 Method of representing yield on a cartographic base map. The shaded area corresponds to the surface (m^2) to which the big bag and the fruit weight value (kg) will be associated. The colour of the area indicates the yield ($kg \cdot m^{-2}$). O is the origin of the cartesian x and y planes. V_1, V_2, V_3 and V_4 are the vertices of the polygon delimiting the harvested area. P_1, P_2, P_n are the cartesian coordinate points where the different big bags are located. α is the angle formed by the line joining P_1 and P_n with the x-plane. β is the angle formed by the side V_1V_3 of the polygon with the x-plane

Map generation procedure

It is necessary to enter a series of parameters into the system before harvesting in order to generate harvest maps. This is done manually using the wireless electronic system display shown in Fig. 3, and Fig. 4 illustrates some of these parameters:

Row width (Rw): distance between tree trunks in the perpendicular direction where the nets are placed.

Tree spacing (Ts): distance between two tree trunks in the perpendicular direction where the bags are placed.

Tree number (Tn): number of trees harvested per row for each storage system. This parameter will depend on the approximate production of the trees, bearing in mind that the capacity of each bag is approximately 200 kg.

Harvesting orientation (Ho): indicates the direction (left or right) in which the fruit is harvested from the storage system.

With each big bag weighed, an information frame containing the parameters mentioned above is recorded in the internal memory. To these parameters are added the geographical coordinates obtained by GNSS RTK (latitude and longitude), the weight value in kilograms, the date and time of registration and a unique identifier that differentiates each big bag weighed (sub-batches). This identifier (Ids) consists of a 10-digit code of random numbers and letters generated by the microcontroller board. When the trailer is full, the operator finishes the logistical operation by pressing on the display to close the batch, which consists of the sum weight of all the big bags. At that moment, each of the information frames previously recorded in the display's internal memory are sent to the cloud application (described in the following section) together with another 10-digit identifier created for the batch (Idb). The batch corresponds to the loaded trailer. The trailer is then transported to the industry, where the fruit batch will be unloaded. Through the developed interface (Fig. 3), it is also possible to consult aspects concerning the GNSS system status, such as reception of georeferencing data, connection to the Networked Transport of RTCM via Internet Protocol (NTRIP) server, correction of coordinates, the status of mobile data connection and status of communication with the electronics on board the trailer.

Cloud-based application for yield estimation

The cloud application was developed in the open source Microsoft.NET framework which allows applications to be created to run natively on any operating system using tools, libraries and languages. It enables the polygons design and registration of plots for the big bags and batches of fruit harvested and representation of the information on a cartographic base map. In the representation, shaded polygons of different colours are generated according to a scale based on the kg m^{-2} weighed at each location during harvesting logistics. The procedure followed for the polygon representation (Fig. 4) was:

1. The big bag and batch identifier parameters (Ids and Idb), Rw, Ts, Tn and Ho were extracted from the database, as were the geographical coordinates in decimal degrees notation of the different locations recorded for each big bag of fruit.
2. The data were associated to a previously created plot. The methodology applied to create the plot and associate the georeferenced points to it was that of Bayano-Tejero et al., 2019.
3. The geographical coordinates recorded in decimal degrees were converted to UTM geographical coordinates (x,y) expressed in metres (Snyder, 1987), obtaining the different points (P_1, \dots, P_n).
4. The r line inclination formed by the initial and final geographical points $P_1 = (x_1, y_1)$ and $P_n = (x_n, y_n)$ with respect to the easting plane (x) was calculated (Eq. 1).

$$\alpha = \arctan\left(\frac{y_n - y_1}{x_n - x_1}\right) \tag{1}$$

5. The vertices $V_{1,n}$, $V_{2,n}$ of the polygon were obtained. To do this, first the distances ($d_{x,v1v2}$, $d_{y,v1v2}$) on both x and y axes were calculated (Eq. 2 and Eq. 3). Then, the coordinates of the two vertices $V_{1,n}$, $V_{2,n}$ were found for each point (P_1, \dots, P_n), one on each side of the point on the r line (Eq. 4 and Eq. 5).

$$d_{x,v1v2} = \frac{R_w}{2} \cdot \cos\alpha \tag{2}$$

$$d_{y,v1v2} = \frac{R_w}{2} \cdot \sin\alpha \tag{3}$$

$$V_{1,n} = (x_{v1,n}, y_{v1,n}) = (x_n - d_{x,v1v2}, y_n - d_{y,v1v2}) \tag{4}$$

$$V_{2,n} = (x_{v2,n}, y_{v2,n}) = (x_n + d_{x,v1v2}, y_n + d_{y,v1v2}) \tag{5}$$

6. The vertices $V_{3,n}$ and $V_{4,n}$ were calculated. For this purpose, the distance on the x and y axis, ($d_{x,v1v3}$, $d_{y,v1v3}$) were calculated (Eq. 6 and Eq. 7).

$$d_{x,v1v3} = T_n \cdot T_s \cdot \cos\beta \tag{6}$$

$$d_{y,v1v3} = T_n \cdot T_s \cdot \sin\beta \tag{7}$$

Travel direction on the xy plane (easting and northing) was then calculated by the difference between the coordinates of points P_1 and P_n . This determined the travel direction on the plane during logistics, and thus the quadrant in which these points were located (Q1–Q4).

$$x_n > x_1 \text{ and } y_n > y_1 \rightarrow Q_1$$

$$x_n < x_1 \text{ and } y_n > y_1 \rightarrow Q_2$$

$$x_n > x_1 \text{ and } y_n < y_1 \rightarrow Q_3$$

$$x_n < x_1 \text{ and } y_n < y_1 \rightarrow Q_4$$

Based on the Q quadrant result and the parameter H_0 , the following equations (Eq. 8–Eq. 15) were applied for calculation of vertex coordinates $V_{3,n}$ and $V_{4,n}$.

If Q_1 and $H_0 = \text{left}$ or Q_3 and $H_0 = \text{right}$, then

$$V_{3,n} = (x_{v1,n} - d_{x,v1v3}, y_{v1,n} + d_{y,v1v3}) \tag{8}$$

$$V_{4,n} = (x_{v2,n} - d_{x,v1v3}, y_{v2,n} + d_{y,v1v3}) \tag{9}$$

If Q_2 and $H_0 = \text{left}$ or Q_4 and $H_0 = \text{right}$, then

$$V_{3,n} = (x_{v1,n} + d_{x,v1v3}, y_{v1,n} - d_{y,v1v3}) \quad (10)$$

$$V_{4,n} = (x_{v2,n} + d_{x,v1v3}, y_{v2,n} - d_{y,v1v3}) \quad (11)$$

If Q_3 and $H_o = \text{left}$ or Q_1 and $H_o = \text{right}$, then

$$V_{3,n} = (x_{v1,n} - d_{x,v1v3}, y_{v1,n} - d_{y,v1v3}) \quad (12)$$

$$V_{4,n} = (x_{v2,n} - d_{x,v1v3}, y_{v2,n} - d_{y,v1v3}) \quad (13)$$

If Q_4 and $H_o = \text{left}$ or Q_2 and $H_o = \text{right}$, then

$$V_{3,n} = (x_{v1,n} + d_{x,v1v3}, y_{v1,n} + d_{y,v1v3}) \quad (14)$$

$$V_{4,n} = (x_{v2,n} + d_{x,v1v3}, y_{v2,n} + d_{y,v1v3}) \quad (15)$$

7. Once the 4 vertices coordinates forming the polygons were calculated, the UTM coordinates were converted to decimal geographical coordinates. For determination of each polygon colour, a scale of 11 colours was defined and intervals in kg m^{-2} were established. The converted georeferenced points defining a polygon and the associated colour were sent to the Google Maps API for representation on a cartographic base map.

8. Subsequently, it is possible to access the cloud application and consult and export the data relating to the plot (batch ID, time, location, weight). To do this, access the IP address of the application with the credentials and select a plot from the drop-down menu to view the map associated with the registered production. A user demo has been created to show the application's utility (Supplementary material).

Tests for assessing the system

To evaluate the performance of the developed system, we conducted different tests of the GNSS system and the loading bolt, in addition to a test under real working conditions.

GNSS system accuracy

The system was statically placed outside in an area with a completely clear sky. Using the U-center v21.05 GNSS system software, geographic coordinates were recorded for 30 min from system start-up to check deviation and accuracy over time. The test was performed with and without receiving RTCM 3.x corrections via NTRIP. The reference base station used for the corrections belonged to the Andalusian Positioning Network (RAP) with identifier CRDB 13461M001 located in Cordoba at coordinates $X = 342,765.562$ m and $Y = 4,193,718.831$ m (UTM coordinates, zone 30S, datum ETRS89), 7200 m as the crow flies from the test location. To compare the accuracy and precision of the system with and without corrections we used the parameter twice the distance root mean squared (2DRMS), which indicates the radius in metres where the GNSS points are located with a probability between 95.4 and 98.2% (Specht, 2021) expressing the accuracy in 2D (Eq. 16).

$$2DRMS = 2 \cdot \sqrt{\sigma_x^2 + \sigma_y^2} \quad (16)$$

σ_x and σ_y are the respective absolute standard errors of the UTM X and Y coordinates with respect to the mean of all points expressed in metres.

The horizontal dilution of precision (HDOP) and horizontal position accuracy (PACC H) parameters were also recorded. HDOP is a measure of the geometric quality of a satellite configuration in the sky and the lower the value the better the accuracy of the estimated horizontal position (latitude and longitude). PACC H is the estimate of horizontal position accuracy calculated during post-processing by the U-center v21.05 software. It indicates the horizontal position accuracy as a function of satellite parameters (Sanna et al., 2022).

Weighing system accuracy

First, it was verified that the installation of the loading bolt was suitable, and the measurements could be realised correctly regardless of the extension and elevation of the telescopic arm. Subsequently, a test was carried out to determine the response of the loading bolt to a constant increase in known weight, considering the variability in big bag weight that may exist between different productive areas of the plots. To this end, 16 weighing measurements were carried out, adding fruits of 15.07 ± 0.06 kg until reaching 240 kg, with 2 repetitions. This limit was set according to the maximum weight that the arm can carry when fully extended. The weight measured by the loading bolt was compared by means of a scale with a resolution of 1 g and a maximum range of 30 kg (PCE-TB30, PCE, Deutschland, Germany).

Performance of the system under real working conditions

The complete system was tested in an intensive olive grove with a square planting layout of 7 m row width and 6.5 m tree spacing, and in a traditional olive grove that also had a square planting layout of 9.5 m row width and 9 m tree spacing. Both plots were in Cordoba, in Lucena (37.392882, - 4.634364) and Aguilar de la Frontera (37.366609, - 4.641397), respectively in slope conditions between 3 and 7%. The plots were registered in the cloud application and harvested with the usual harvesting procedure, adapted to the logistics explained above. The process was carried out over an area of 1.8 ha in the case of the intensive olive grove and 2.35 ha for the traditional olive grove. The big bags were handled by operators qualified to carry out this task.

Results

GNSS system accuracy

Figures 5a and b show the accuracy of the georeferencing system. In Fig. 5a we observe that the 2DRMS of the system with corrections is much lower than the values calculated without corrections (0.58 and 1.82 m, respectively) measured from initial start-up. Figure 5b shows that the system with corrections becomes highly accurate very quickly after receiving the corrections, stabilising within 10 s of start-up. However, the system without corrections requires more time, around 250 s.

Considering only the recorded data and once both GNSS systems had stabilised, the accuracy and precision are considerably reduced with a 2DRMS value of 0.019 m for the system with corrections and 0.59 m without corrections. Considering the errors in terms of

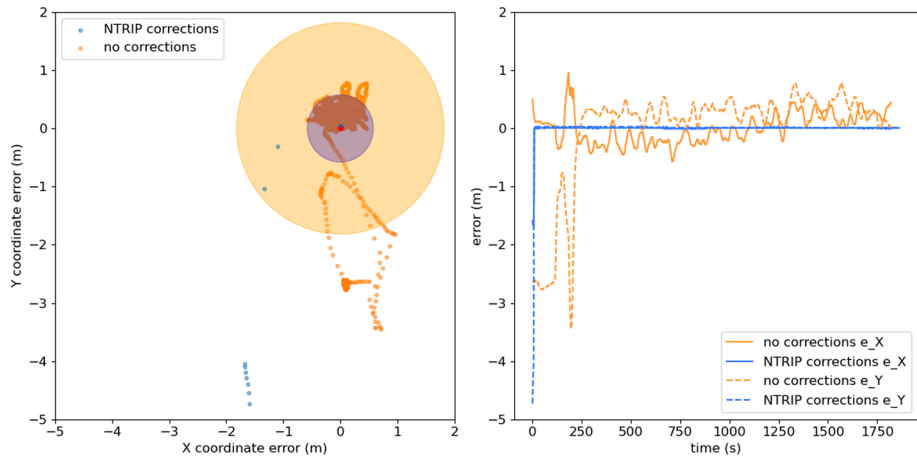


Fig. 5 Circle determining the accuracy of the GNSS system with 95.4–98.2% accuracy (left). For the GNSS system with NTRIP corrections most points are in the centre of the blue circle, below the red dot. Evolution over time of error in UTM X and Y coordinates (right). The evolution of the X and Y errors over time with NTRIP corrections is similar, and the lines overlap

the X and Y coordinates (e_X , e_Y), the system with corrections presents an average error in X and Y of 0.008 ± 0.005 m and 0.017 ± 0.008 m respectively. The system without corrections presents an average error in X and Y of -0.018 ± 0.24 m and 0.31 ± 0.17 m, respectively. The HDOP and PACC H parameters took values of 0.53 ± 0.049 and $0.014 \pm 4.32e-16$ m, respectively for the system with corrections, which indicates good satellite data reception and therefore a good accuracy estimation. For the system without corrections, the HDOP and PACC parameters were 0.57 ± 0.047 and 0.308 ± 0.004 m, respectively.

Weighing system accuracy

Figure 6 illustrates the weighing system's relative error. This remained stable, although there was a slight decrease as the weight measured by the loading bolt increased. The mean absolute error was 1.1 ± 0.99 kg. The higher relative errors measured at the beginning of the weighing process were due to the low weight in the big bag and the resolution of the loading bolt (0.5 kg) compared to the scale (1 g). Therefore, the weighing system gives high accuracy for the amount of fruit that the big bags will contain in the harvesting process, between 50 and 240 kg approximately.

Results of work in real conditions

The average time measured for loading and unloading operations between the different big bags was 154.05 ± 31.49 s for the intensive olive grove and 158.50 ± 24.85 s for the traditional olive grove. In addition to this, we have to consider the time it takes to transport the fruit to the final harvesting point, once the trailer reaches full capacity or when another batch is to be started. This time will vary depending on the location of the plot from the industry or the intermediate harvesting point. Table 1 provides the batch data recorded for each planting system. Two batches of fruit per main row were estimated for

Fig. 6 Relative error of the load bolt to the scale. Black line indicates the linear regression model fit. Gray area indicates a 95% confidence interval

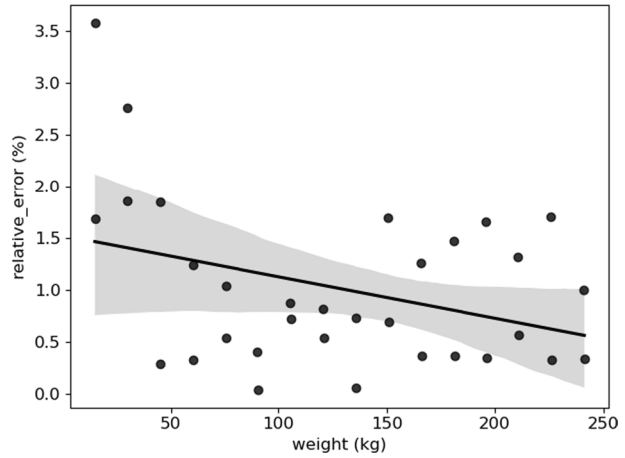


Table 1 Information recorded for the batches during the tests for intensive and traditional olive groves

Planting system	Tree distances (m)	Batch ID	Weight (kgD)	Date and time
Intensive	7*6.5	J56APFT625	1430.5	2022-11-29 09:09:29
		OJ8DFG190A	1321.5	2022-11-29 09:49:56
		HJW547HEN0	1535.5	2022-11-29 10:29:41
		HFT787T45N	1414	2022-11-29 11:11:13
		H677UYKYU1	1716	2022-11-29 11:53:06
		46TRHG87AS	1257	2022-11-29 12:30:15
		GY876E4B67	1276.5	2022-11-29 13:15:27
		D56GHFGJGG	1351	2022-11-29 13:44:11
Traditional	9,5*9	A65JHSZG47	1229.5	2022-12-05 09:53:39
		05DFG6H7V4	1603	2022-12-05 10:34:47
		5YGFDYK5GF	1417	2022-12-05 11:07:11
		6766ERBGTY	1470.5	2022-12-05 11:44:58
		CEPK40ITJB	1270.5	2022-12-05 12:24:46
		W5605GFBDF	1469.5	2022-12-05 13:03:11
		1KKLUGGD45	1358	2022-12-05 13:37:32
		J4GE45IUIL	1336	2022-12-05 14:12:44

each of the two plots so that the trailers did not reach their full capacity for each batch, thus avoiding batches that had very unequal weights.

The cloud application generated the harvest maps, which were checked to ensure that they correctly represented the information (Figs. 7 and 8). It is possible to consult each of the big bags corresponding to each batch with its respective ID, weight and geographical coordinates by means of the batch ID (Table 1) through the user demo (supplementary material). Thus, it is possible to maintain traceability of the fruit. We observe a greater variability of colours in the harvest map generated for intensive olive groves, which indicates a greater variability in production between each of the different areas. The average production in this case was $0.66 \pm 0.15 \text{ kg} \cdot \text{m}^{-2}$. In the case of the



Fig. 7 Yield map generated in the cloud application for the intensive orchard

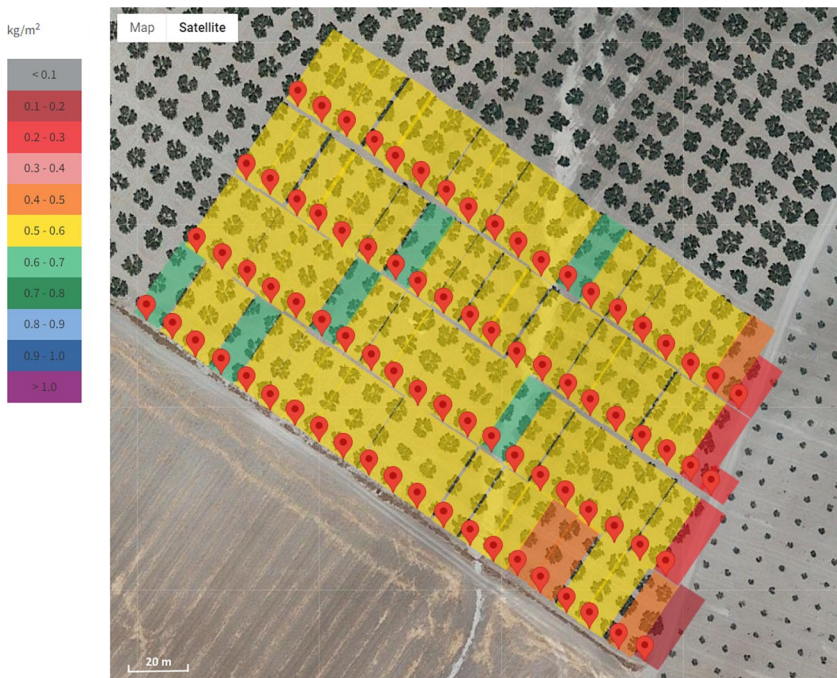


Fig. 8 Yield map generated in the cloud application for the traditional orchard

traditional olive grove, production between the different zones was much more stable, with an average production of $0.55 \pm 0.08 \text{ kg}\cdot\text{m}^{-2}$. In both planting systems, we see that the least productive areas were in the rows adjacent to where the plot bordered with roads or gullies.

Discussion

The GNSS system with NTRIP corrections showed a high accuracy of around 20 mm. The initial deviations had a short time duration (10 s) and were due to system start-up, reception of georeferencing data, and corrections via connection to the NTRIP network. This aspect has no influence for the developed application since the operation mode is continuous and does not require switching the electronic system off and, if it is, the time required for stabilisation and provision of reliable data is assumable. In the case of the GNSS system without corrections, accuracy and precision were lower, and the time taken to provide more reliable data was longer (250 s). After this time, the system could also be used for the developed application as the error measured in X and Y is less than half the width of a row (3–3.5 m for intensive and 4–6 m for traditional) where the trailer runs. In this way, there is no risk of locating the polygon in another row or main row in the cloud application. However, without corrections, the different polygons would not be as well aligned with each other or arranged on the map as is the case when corrections are used. Even so, the GNSS system without corrections, also needs to be valid in these circumstances with regard to results obtained (Fig. 5), since the absence of mobile coverage is common in some rural areas (Cabrera-Castellanos et al., 2021). On the other hand, the time spent with the device switched on will influence obtaining better accuracy and precision in the geographic coordinates, so this is a factor to consider when there are no corrections (Valbuena et al., 2010). If greater accuracy is required, a base station could be located on the plot to send corrections to the system on board the trailer (Berber et al., 2012). Finally, the spatial distribution of the satellites in the sky above the measurement point was good as indicated by the HDOP parameter and this is also a factor that influences the accuracy of the coordinates obtained. (Hussain et al., 2020). However, there are several additional factors that affect the accuracy of a GNSS system, such as the number of satellites, multipath effects, ionospheric delay, the number of satellites, tree coverage, terrain slope or cloudiness of the sky, among others (Feng et al., 2021; Zuo et al., 2019).

The weighing system had an average absolute error of around 1 kg, which is low in accordance with the amount of fruit the big bags can carry. This allows small farmers and traditional olive growers to monitor their production very precisely. The telescopic arm used cannot handle more than 300 kg with the arm fully extended, although systems with a higher load capacity are available on the market. The loading bolt resolution (0.5 kg) resulted in less accurate results at the beginning of the tests with low weights and constant weight increments (15 kg). However, the error is negligible for higher weights such as can occur in traditional and intensive olive orchards, where the average production per tree is 60 kg and 20 kg, respectively (Fernández-Escobar et al., 2013; Lo Bianco et al., 2021).

The generated harvest or yield maps and their associated colours provide a quick overview of productivity differences between different areas of the plot. However, the maps are made in a discrete way, in line with the logistics used in many plantations, unlike other harvest maps that are generated with the continuous work of machinery (Maja and Ehsani, 2010) or by drones (Stateras and Kalivas, 2020). A future improvement would aim to

automatically create continuous interpolated yield maps, but would require a number of corrections and extra programming to display the information reliably.

The harvest maps generated were recorded in the database together with the olive orchard season, which forms a production history and allows the farmer to make a comparison with future maps of the same plot. This helps in decision-making about plantation management and in verification of the evolution over successive seasons. It also allows production comparisons between plots with different crop types, tree densities and different management methods (Vieri and Sarri, 2010).

The developed system is applicable to other crops that use square or rectangular planting layouts such as the almond or apple (Pantera et al., 2018). However, the proposed algorithm for polygon generation requires a square or rectangular planting layout for proper operation. For its application in irregular planting systems or in another configuration such as quincunx spacing (Javaid et al., 2017), the representation of the maps would not be reliable. This is due to the fact that the trees would not be aligned along contiguous rows, and it would be necessary to modify the proposed algorithm to obtain other polygon types.

The proposed electronic system and cloud application are adapted to the logistic system used in plantations that use big bags and trailers with an arm to load fruit. By means of the display, the system can be adapted to different field conditions such as the number of trees for each big bag and the planting layout of the plot. The designed loading and weighing system is independent of the telescopic arm, so it would be easy adaptable to another system. The loading system could be modified to other systems that handle boxes or use other means of fruit logistics, such as the tomato or pepper (Ahumada and Villalobos, 2011), following the methodology and instrumentation presented in this work.

The logistic process times between loading and unloading one big bag and moving on to the next were short, around 2.5 min. Therefore, the proposed system does not alter the workflow of operators as they only need to configure the display at the beginning of the logistic process or in the case of changes in the planting layout, harvesting direction or boundary rows of the plot, which usually have fewer trees. Even so, the interface is user-friendly, and configuration takes only a few seconds. Furthermore, the proposed procedure with big bags has the advantage that the harvesting and the logistics processes can be performed separately, i.e., fruit loading can be conducted in parallel or in series at any time, with the advantage that this brings in avoiding delays. With the operating times measured, full capacity of the trailer can be reached in around 30 min in the case of big bags with approximately 200 kg of fruit. Although it is possible that trailer capacity may not be fully reached due to weight differences between the big bags, the equidistant arrangement in space of the big bags and their association with the number of trees allows the acquisition of accurate yield maps. Other research shows proposals that are less close to reality as they are based on the average harvest for an area where the big bags are unevenly distributed (Fountas et al., 2011).

The proposed system also makes it possible to record the traceability of fruit batches thanks to an alphanumeric code associated with each big bag and the geographical coordinates. In addition, the entire batch or trailer carries another code associated with the respective codes of the big bags that constitute it. In this way, it is possible to ascertain which plot area a batch came from and take the appropriate decisions in the case of detected anomalies. For a traditional olive grove with an average production between 3500 and 6000 kg ha⁻¹, depending on whether it is rainfed or irrigated, a complete trailer can correspond to an area between 0.33 and 0.57 ha. In the case of intensive olive groves with an average production between 5000 and 10000 kg ha⁻¹, the trailer will correspond to an area between 0.2 and 0.4 ha (AEMO, 2020). The traceability control of the harvest is an

added value to the product that could help revalue some plantation systems currently suffering gradual decline, as is the case of traditional olive groves (Fernández-Escobar et al., 2013).

Crop yield monitoring systems are usually expensive. In this case, the developed system is adaptable to a trailer that the producer usually has for different tasks. The cost of the complete system including all necessary elements (control operated arm, battery, loading bolt, T-shaped implement and display) is around €5000. This makes it possible for small producers, who cannot afford other, high cost harvesting and logistics machinery, to implement the developed system on small farms.

Conclusions

A yield monitor was developed for small producers based on a trailer with a manipulator arm equipped with a mechanical implement that allows the loading of big bags for olives. In addition, the yield monitor has an electronic system for weighing and geo-referencing the fruit batches. The data from the harvested batches are recorded in a cloud application that generates yield maps of the plot in a farmer-friendly way, and allows traceability of the harvested fruit batches. The geo-referencing and weighing systems were tested and reported very low error, which proves they are a valid option for the developed application. The complete system was used in real field conditions in both a traditional olive grove and an intensive olive grove with low logistic times according to the methodology described. The harvest maps generated for both plots provided an adequate visualisation of production that can be of great use for its management, either as a comparison between plots, or to control its historical evolution.

Supplementary Information The online version contains supplementary material available at <https://doi.org/10.1007/s11119-023-10078-w>.

Acknowledgements The authors are grateful for the funding received by the Consejería de Conocimiento, Investigación y Universidad (Junta de Andalucía) under the PYC20 RE 024 UCO Project 'Development of an IoT application to monitor the harvest performed by different mechanization systems in traditional olive harvesting for the improvement of its management and traceability'. We would also like to thank Juan Pérez-Moya for the support given in the design of the cloud application.

Funding Consejería de Economía, Conocimiento, Empresas y Universidad, Junta de Andalucía, PYC20 RE 024 UCO, Sergio Bayano-Tejero

Data Availability Not applicable.

References

- AEMO (2020). Aproximación a los costes del cultivo del olivo. Desarrollo y conclusiones del estudio AEMO.
- Ahumada, O., & Villalobos, J. R. (2011). Operational model for planning the harvest and distribution of perishable agricultural products. *International Journal of Production Economics*, 133, 677–687. <https://doi.org/10.1016/j.ijpe.2011.05.015>
- Ampatzidis, Y. G., & Vougioukas, S. G. (2009). Field experiments for evaluating the incorporation of RFID and barcode registration and digital weighing technologies in manual fruit harvesting. *Computers and Electronics in Agriculture*, 66, 166–172. <https://doi.org/10.1016/j.compag.2009.01.008>

- Ampatzidis, Y. G., Vougioukas, S. G., Whiting, M. D., & Zhang, Q. (2014). Applying the machine repair model to improve efficiency of harvesting fruit. *Biosystems Engineering*, *120*, 25–33. <https://doi.org/10.1016/j.biosystemseng.2013.07.011>
- Ampatzidis, Y., Tan, L., Haley, R., & Whiting, M. D. (2016). Cloud-based harvest management information system for hand-harvested specialty crops. *Computers and Electronics in Agriculture*, *122*, 161–167. <https://doi.org/10.1016/j.compag.2016.01.032>
- Bayano-Tejero, S., Sola-Guirado, R. R., Gil-Ribes, J. A., & Blanco-Roldán, G. L. (2019). Machine to machine connections for integral management of the olive production. *Computers and Electronics in Agriculture*, *166*, 104980. <https://doi.org/10.1016/j.compag.2019.104980>
- Berber, M., Ustun, A., & Yetkin, M. (2012). Comparison of accuracy of GPS techniques. *Measurement*, *45*, 1742–1746. <https://doi.org/10.1016/j.measurement.2012.04.010>
- Cabrera-Castellanos, D. F., Aragón-Zavala, A., & Castañón-Ávila, G. (2021). Closing connectivity gap: An overview of mobile coverage solutions for not-spots in rural zones. *Sensors*, *21*, 8037. <https://doi.org/10.3390/s21238037>
- Colaço, A. F., Trevisan, R. G., Karp, F. H. S., & Molin, J. P. (2020). Yield mapping methods for manually harvested crops. *Computers and Electronics in Agriculture*. <https://doi.org/10.1016/j.compag.2020.105693>
- Feng, A., Zhou, J., Vories, E. D., Sudduth, K. A., & Zhang, M. (2020). Yield estimation in cotton using UAV-based multi-sensor imagery. *Biosystems Engineering*, *193*, 101–114. <https://doi.org/10.1016/j.biosystemseng.2020.02.014>
- Feng, T., Chen, S., Feng, Z., Shen, C., & Tian, Y. (2021). Effects of canopy and multi-epoch observations on single-point positioning errors of a GNSS in coniferous and broadleaved forests. *Remote Sensors*, *13*, 2325. <https://doi.org/10.3390/rs13122325>
- Ferguson, L. (2006). Trends in olive fruit handling previous to its industrial transformation. *Grasas y Aceites*, *57*, 9–15. <https://doi.org/10.3989/gya.2006.v57.i1.17>
- Fernández-Escobar, R., de La Rosa, R., Leon, L., Gómez, J. A., Testi, L., Orgaz, F., Gil-Ribes, J. A., Quesada-Moraga, E., & Trapero, A. (2013). Present and future of the Mediterranean olive sector Evolution and sustainability of the olive production systems. *Options Méditerranéennes*, *A*, *42*, 11–41.
- Fountas, S., Aggelopoulou, K., Bouloulis, C., Nanos, G. D., Wulfsohn, D., Gemtos, T. A., Paraskevopoulos, A., & Galanis, M. (2011). Site-specific management in an olive tree plantation. *Precision Agriculture*, *12*, 179–195. <https://doi.org/10.1007/s11119-010-9167-4>
- Fulton, J., Hawkins, E., Taylor, R., & Franzen, A. (2018). Yield monitoring and mapping. *Precision Agriculture Basics*. <https://doi.org/10.2134/precisionagbasics.2016.0089>
- García, J. M., & Yousfi, K. (2006). The postharvest of mill olives. *Grasas y Aceites*, *57*, 16–24. <https://doi.org/10.3989/gya.2006.v57.i1.18>
- Gené-Mola, J., Gregorio, E., Auat Cheein, F., Guevara, J., Llorens, J., Sanz-Cortiella, R., Escolà, A., & Rosell-Polo, J. R. (2020). Fruit detection, yield prediction and canopy geometric characterization using LiDAR with forced air flow. *Computers and Electronics in Agriculture*, *168*, 105121. <https://doi.org/10.1016/j.compag.2019.105121>
- Guevara, L., Rocha, R. P., & Cheein, F. A. (2021). Improving the manual harvesting operation efficiency by coordinating a fleet of N-trailer vehicles. *Computers and Electronics in Agriculture*, *185*, 106103. <https://doi.org/10.1016/j.compag.2021.106103>
- Hussain, A., Ahmed, A., Magsi, H., & Tiwari, R. (2020). Adaptive GNSS receiver design for highly dynamic multipath environments. *IEEE Access*, *8*, 172481–172497. <https://doi.org/10.1109/ACCESS.2020.3024890>
- Jadhav, U., Khot, L. R., Ehsani, R., Jagdale, V., & Schueller, J. K. (2014). Volumetric mass flow sensor for citrus mechanical harvesting machines. *Computers and Electronics in Agriculture*, *101*, 93–101. <https://doi.org/10.1016/j.compag.2013.12.007>
- Javaid, K., Qureshi, S. N., Masoodi, L., & Sharma, P. (2017). Orchard designing in fruit crops. *J. Pharmacogn. Phytochem.*, *6*, 1081–1091.
- Lo Bianco, R., Proietti, P., Regni, L., & Caruso, T. (2021). Planting systems for modern olive growing: strengths and weaknesses. *Agriculture*, *11*, 494. <https://doi.org/10.3390/agriculture11060494>
- Longchamps, L., Tisseyre, B., Taylor, J., Sagoo, L., Momin, A., Fountas, S., & Khosla, R. (2022). Yield sensing technologies for perennial and annual horticultural crops: a review. *Precision Agriculture*. <https://doi.org/10.1007/s11119-022-09906-2>
- Maja, J. M., & Ehsani, R. (2010). Development of a yield monitoring system for citrus mechanical harvesting machines. *Precision Agriculture*, *11*, 475–487. <https://doi.org/10.1007/s11119-009-9141-1>
- Mizushima, A., & Lu, R. (2013). A low-cost color vision system for automatic estimation of apple fruit orientation and maximum equatorial diameter. *Transactions of the ASABE*, *56*, 813–827. <https://doi.org/10.13031/trans.56.9343>

- Pantera, A., Burgess, P. J., Mosquera Losada, R., Moreno, G., López-Díaz, M. L., Corroyer, N., McAdam, J., Rosati, A., Papadopoulos, A. M., Graves, A., Rigueiro Rodríguez, A., Ferreiro-Domínguez, N., Fernández Lorenzo, J. L., González-Hernández, M. P., Papanastasis, V. P., Mantzanas, K., Van Lerberghe, P., & Malignier, N. (2018). Agroforestry for high value tree systems in Europe. *Agroforestry Systems*, 92, 945–959. <https://doi.org/10.1007/s10457-017-0181-7>
- Perez-Ruiz, M., Martínez-Guante, J., & Upadhyaya, S. K. (2021). High-precision GNSS for agricultural operations. *GPS and GNSS Technology in Geosciences*. Amsterdam: Elsevier.
- Plasquy, E., Sola-Guiraldo, R. R., Florido, C., García, J. M., & Blanco-Roldán, G. (2019). Evaluation of a manual olive fruit harvester for small producers. *Research in Agricultural Engineering*, 65, 105–111. <https://doi.org/10.17221/18/2019-RAE>
- Plasquy, E., Florido, M. C., Sola-Guirado, R. R., & García, J. M. (2021). Effects of a Harvesting and conservation method for small producers on the quality of the produced olive oil. *Agriculture*, 11, 417. <https://doi.org/10.3390/agriculture11050417>
- Sanna, G., Pisanu, T., & Garau, S. (2022). Behavior of low-cost receivers in base-rover configuration with geodetic-grade antennas. *Sensors*, 22, 2779. <https://doi.org/10.3390/s22072779>
- Snyder, J. P. (1987). Map projections. *Scottish Geographical Magazine*, 6, 57–61. <https://doi.org/10.1080/14702549008554700>
- Sola-Guirado, R. R., Castro-García, S., Blanco-Roldán, G. L., Jiménez-Jiménez, F., Castillo-Ruiz, F. J., & Gil-Ribes, J. A. (2014). Traditional olive tree response to oil olive harvesting technologies. *Biosystems Engineering*, 118, 186–193. <https://doi.org/10.1016/j.biosystemseng.2013.12.007>
- Specht, M. (2021). Determination of navigation system positioning accuracy using the reliability method based on real measurements. *Remote Sensing*, 13, 4424. <https://doi.org/10.3390/rs13214424>
- Stateras, D., & Kalivas, D. (2020). Assessment of olive tree canopy characteristics and yield forecast model using high resolution UAV imagery. *Agriculture*, 10, 385. <https://doi.org/10.3390/agriculture10090385>
- Stein, M., Bargoti, S., & Underwood, J. (2016). Image based mango fruit detection, localisation and yield estimation using multiple view geometry. *Sensors*, 16, 1915. <https://doi.org/10.3390/s16111915>
- Underwood, J. P., Hung, C., Whelan, B., & Sukkarieh, S. (2016). Mapping almond orchard canopy volume, flowers, fruit and yield using lidar and vision sensors. *Computers and Electronics in Agriculture*, 130, 83–96. <https://doi.org/10.1016/j.compag.2016.09.014>
- Valbuena, R., Mauro, F., Rodríguez-Solano, R., & Manzanera, J. A. (2010). Accuracy and precision of GPS receivers under forest canopies in a mountainous environment. *Spanish Journal of Agricultural Research*, 8, 1047. <https://doi.org/10.5424/sjar/2010084-1242>
- Vieri, M., & Sarri, D. (2010). Criteria for introducing mechanical harvesting of oil olives: results of a five-year project in central Italy. *Advances in Horticultural Science*, 24, 78–90.
- Zuo, X., Bu, J., Li, X., Chang, J., & Li, X. (2019). The quality analysis of GNSS satellite positioning data. *Cluster Comput.*, 22, 6693–6708. <https://doi.org/10.1007/s10586-018-2524-1>

Publisher's Note Springer Nature remains neutral with regard to jurisdictional claims in published maps and institutional affiliations.

Springer Nature or its licensor (e.g. a society or other partner) holds exclusive rights to this article under a publishing agreement with the author(s) or other rightsholder(s); author self-archiving of the accepted manuscript version of this article is solely governed by the terms of such publishing agreement and applicable law.